Variable Admittance Control of Robot Manipulators Based on Human Intention

Gitae Kang, Hyun Seok Oh, Joon Kyue Seo, Uikyum Kim, and Hyouk Ryeol Choi, *Fellow, IEEE*

***Abstract*—This paper presents a variable admittance control method to achieve intuitive human–robot interactions that consider human intentions. Human intention is classified into two categories—direct and indirect. With respect to direct intention, the concept of standard force is introduced to adjust the interacting force. The proposed variable admittance control method improves intuitiveness when velocity is used as an estimate of direct intention. In the estimation of indirect intention, a force guidance method is suggested to make a robot follow and guide a human. The proposed control methodology is adapted to a six-DOF manipulator based on a one-dimensional analysis. The experiments are conducted with a manipulator (Universal Robots, UR10) and a force/torque sensor (Robotus, RFT60-HA) to evaluate the performance. The experiments validate that variable admittance control enhances the execution time, accuracy, and comfort of the operator.**

***Index Terms*—Admittance control, human intention, physical human–robot interaction, variable admittance.**

I. Introduction

INTERACTION between humans and robots has become increasingly important as robots begin to share spaces with humans. Specifically, physical human–robot interaction is a promising application in various fields such as haptics, teleoperation, robotic surgery, etc. Collaboration between humans and robots by guaranteeing safety improves work environments and efficiency.

Direct teaching is a well known function of physical human–robot interaction. The robot moves based on the intentions of the human through the use of human force and torque. Direct teaching is based on the "impedance controller," which typically refers to both impedance and admittance controls [1]. The impedance controller is a control system that inputs displacement and outputs force. In contrast, the admittance controller is a control system that inputs force and outputs displacement. The admittance controller has several advantages that can be easily adapted to the current industrial robot system, namely the position-controlled system. Additionally, the admittance controller interacts with a stiff environment with robustness to stiction effects [2].

In teleoperation systems specifically, the impedance and admittance controllers are actively investigated for human–robot interactions, including direct teaching. A state-of-the-art controller for teleoperation systems can be classified according to the focus of the controller. A controller may be environment-related, operator-related, or task-related [3]. In an environment-related controller, variable admittance is only applied to contact with environments [4], not human intention. The task-related controller focuses on specific tasks [5], such as peg-in-hole, obstacle avoidance, or tracking. The operator-related controller only considers online human intentions.

In an operator-related controller, various control methods are proposed to improve stability and intuitiveness. Based on the early studies by Colgate and Hogan [6], [7], an estimation of human arm impedance was used for the variable impedance controller [8]–[10]. The analytical model of the robot and the human arm was calculated and the admittance parameters were adjusted relative to the stiffness of the human arm. Similarly, in [11] and [12], the minimum jerk model was proposed to estimate human motion. However, this requires the analytic model in advance, and the estimation is not accurate because of the simplification of the model.

Conversely, several approaches used sensor data and state information to adjust admittance parameters. In [13], Dimeas and Aspragathos used an online fuzzy inference system (FIS) that determines the variable damper to minimize the jerk. However, the minimum jerk alone is not sufficient to represent human intentions. In addition, the use of biosignals, namely electromyography (EMG) signals, allows for the use of the measurement of muscle activation for variable admittance control [14]. In this control scheme, the admittance cannot be changed continuously. In a few studies, impedance and admittance varied with the sensor information by considering velocity and acceleration [15], [16]. These approaches estimated human intention with the sensor and state information and adjusted the admittance continuously. However, the adjustment equations of the admittance have been determined experimentally without any standard. This means that these equations cannot be universally applied to other hardware; hence, we need empirical coefficients (α, β [15], a, b [16]) depending on the hardware. Therefore, criteria need to be defined for universal application and thus, form the first issue addressed in this study.

Manuscript received January 22, 2018; revised October 24, 2018; accepted March 23, 2019. Date of publication April 11, 2019; date of current version June 14, 2019. Recommended by Technical Editor Q. Wang. This research was supported by a grant(code R2016001) from Gyeonggi Technology Development Program funded by Gyeonggi Province. *(Corresponding author: Hyouk Ryeol Choi.)*

The authors are with the School of Mechanical Engineering, Sungkyunkwan University, Seoburo 2066, South Korea (e-mail: kkt121@skku.edu; ohs0201@skku.edu; wehhh@skku.edu; krcce@me.skku.ac.kr; hrchoi@me.skku.ac.kr).

Color versions of one or more of the figures in this paper are available online at http://ieeexplore.ieee.org.

Digital Object Identifier 10.1109/TMECH.2019.2910237

Additionally, previous studies mainly considered the instant intention of a human as opposed to a long-term intention. In a task-related controller, virtual fixtures [17], [18] and potential fields [19] are used similar to the long-term intention in haptic systems. The virtual fixtures are applied to guide the human motion along a predefined path or to prevent movement to certain regions. Similarly, the potential fields guide human movement for obstacle avoidance in certain environments. However, these methods use predefined paths, regions, and environments, without considering human online intentions. Accordingly, a method that reflects human online intentions is the second issue considered in this study.

In this study, two variable admittance schemes are introduced for a position-controlled manipulator that enables free motion and precise plane motion based on human intention. In the first scheme, variable admittance for direct intention is proposed. In a manner similar to previous studies, damping is changed for fast and accurate motion by estimating direct intention. Unlike previous studies, the concept of a standard force is applied to the algorithm and is universally applicable to other hardware. In the second scheme, variable admittance for indirect intention is introduced. The admittance is changed to guide a human, similar to the virtual fixture guidance method. The difference is that the proposed force guidance method is able to predict the next human movement online and guide it with variable admittance. The proposed schemes are evaluated with experiments by using a manipulator (Universal Robots, UR10) and a force/torque sensor (Robotus, RFT60-HA). The experimental results show that variable admittance control improves human–robot interactions.

This paper is organized as follows. The background of variable admittance control is explained in Section II. A variable admittance controller for direct intention is introduced in Section III. In Section IV, a variable admittance controller for indirect intention is proposed. Experiments and results are discussed in Sections V and VI, and finally conclusions are presented in Section VII.

II. Background of Variable Admittance Control

A. Admittance Control Model

In a single-dimensional dynamic system, the dynamics equation is expressed as

$$m(\ddot{x} - \ddot{x}_0) + c(\dot{x} - \dot{x}_0) + k(x - x_0) = F_{\text{ext}} \tag{1}$$

where the positive constants m, c, and k represent virtual mass, damping, and stiffness, respectively. Additionally, x, $\dot{x}$, and $\ddot{x}$ represent the position, velocity, and acceleration, respectively. Thus, x_0 indicates the equilibrium position and F_{ext} indicates the external force of the environment.

With respect to direct teaching, virtual spring k and virtual equilibrium position x_0 are assumed to be zero as follows:

$$k = 0$$
$$x_0 = \dot{x}_0 = \ddot{x}_0 = 0. \tag{2}$$

Driving force F_s corresponds to the value of a force/torque sensor as an external force of the environment. The control equation is rewritten as

$$m\ddot{x} + c\dot{x} = F_s. \tag{3}$$

In a manner similar to the velocity control in [15], the desired velocity is derived from (3). Velocity and acceleration are represented as follows:

$$\dot{x}_d(k) = \frac{F_s(k) - c\dot{x}_d(k-1)}{m}T + \dot{x}_d(k-1)$$
$$\ddot{x}_d(k) = \frac{F_s(k) - c\dot{x}_d(k-1)}{m} \tag{4}$$

with respect to a time step k; $\dot{x}_d(k)$ and $\ddot{x}_d(k)$ correspond to the desired velocity and acceleration, respectively. Furthermore, $F_s(k)$ denotes the force measured from the sensor and T denotes the period of the system.

From (5), the relationship between velocity and force is obtained. When the force is constant, velocity converges to a certain value. $\dot{x}_d(k)$ is equal to $\dot{x}_d(k-1)$ and $F_s(k) - c\dot{x}_d(k-1)$ should be zero. The maximum velocity is expressed as

$$\dot{x}_{\max} = \frac{F_s}{c}. \tag{5}$$

The converged velocity is proportional to the force. However, the influence of the force is lower because the interacting force by a human has a limited range. Therefore, as shown by several studies, damping is the main factor with respect to the velocity that affects human perception [20].

Acceleration, expressed as

$$\ddot{x} = \frac{F_s - c\dot{x}}{m} \tag{6}$$

represents the response speed of interaction. Acceleration exhibits a reverse relation with the mass. This implies that a smaller mass leads to a faster response although it also decreases the stability. Therefore, it is necessary to select a proper value that satisfies response speed and stability.

Previous studies reveal few common observations. With a given damping, experimental results indicate that a minimal virtual mass exists for vibration in a stiff environment. Furthermore, the higher virtual mass-to-damping ratio decreases intuitiveness [21], [22].

B. Human Intention

Estimating human intention is the most important issue in the physical human–robot interaction. However, the definition of human intention is used in a wide range of meaning. In previous studies, many researchers use human intention for the instant response as acceleration and deceleration of the robot [12], [22]. In contrast, some researchers use human intention for specific situations and motion such as human–robot handshaking [23] or predefined path [5]. From previous studies, human intention can be divided into two categories, namely, direct intention and indirect intention. Direct intention indicates the instant response from the human force. In contrast, indirect intention implies a long-term purpose of the human such as straight or curve motion. They can be summarized as follows.

1) Direct Intention: Essentially, admittance control corresponds to the response of the direct intention. However, constant admittance shows an inverse relationship between the response time and the accuracy of the manipulator. To improve the performance, admittance should be changed according to the intentions of the human. In previous studies, variable admittance control was proposed to improve the response and accuracy of interaction.

2) Indirect Intention: The estimation of direct intention provides intuitiveness, but it includes sensor noise and human errors. A human is unable to move his/her hand in a precise manner per his/her expectations, and unexpected mistakes occur at times during admittance control. To compensate for unexpected mistakes, variable admittance allows a manipulator to assist humans by force guiding the robot along an expected path, such as linear or curve motion, which represents the indirect intention of a human.

III. Variable Admittance for Direct Intention

With respect to constant admittance control, the response time and the accuracy of control exhibit an inverse relationship. With respect to a certain force and higher damping, the velocity is relatively low and moves slowly. When an operator requires fine manipulation, higher damping is essential for precise movement with low velocity. Conversely, with respect to a certain force and lower damping, the velocity is relatively high and moves fast. When the operator requires a larger movement, lower damping is appropriate to obtain a fast movement with a high velocity.

The main purpose of variable admittance control corresponds to the comfort of a human. The comfort is mainly affected by the interacting force. If an operator wants a fast movement with high damping, the operator needs a high force that makes the operator uncomfortable. In contrast, if the operator requires a fine movement with low damping, it is difficult to control with a low force because of the high virtual mass-to-damping ratio. That is, when the operator controls with a low force, the influence of the inertia is what makes the operator uncomfortable. Consequently, to control a large range of velocity, the usage of a specific force makes the operator more comfortable. The specific force is set as a standard force F_{std}. The standard force depends on each individual and hardware.

A. Variable Damping

From (5), with respect to a constant external force, the maximum velocity depends on the inverse of virtual damping. This means that the minimum force to maintain the velocity is equal to the product of velocity and virtual damping, such as $F_{\min} = \dot{x}c$. To maintain the minimum force in the desired area, it is necessary to decrease virtual damping along with the increase in the velocity. Finally, the variable damping equation is determined as follows:

$$c(\dot{x}) = \frac{F_{\text{std}}}{|\dot{x}|} \quad (\max = c_{\max}, \min = c_{\min}) \tag{7}$$

where maximum and minimum damping correspond to $c_{\max}$ and $c_{\min}$ Ns/m, respectively. Additionally, F_{std} represents the standard force. The parameters are changed based on the hardware and the operator.

In the bounded range of damping, maximum velocity depends on the relation between the external force F_s and the standard force F_{std}. From (5) and (6), maximum velocity and acceleration are rewritten as follows:

$$\dot{x}_{\max} = \frac{F_s}{c} = \frac{F_s}{F_{\text{std}}}|\dot{x}| \tag{8}$$

$$\ddot{x} = \frac{F_s - c\dot{x}}{m} = \frac{F_s - F_{\text{std}}}{m} \tag{9}$$

$$\begin{aligned} F_s = F_{\text{std}} &\Rightarrow \dot{x}_{\max}(-) \\ F_s > F_{\text{std}} &\Rightarrow \dot{x}_{\max}(\uparrow) \\ F_s < F_{\text{std}} &\Rightarrow \dot{x}_{\max}(\downarrow). \end{aligned} \tag{10}$$

When the external force is equal to the standard force, the acceleration is zero and the velocity converges to its maximum. When the external force exceeds the standard force, acceleration is positive and velocity increases. In contrast, when the external force is smaller than the standard force, acceleration is negative and velocity decreases. The proposed variable damping allows the operator to control velocity with a similar magnitude of the force.

To verify the proposed variable damping, simple analyses are conducted in a single-dimensional system. The upper bound of virtual damping $c_{\max}$ corresponds to 60 Ns/m and the lower bound of virtual damping $c_{\min}$ corresponds to 20 Ns/m. The standard force F_{std} set includes 2 and 3 N.

Fig. 1(a) shows a comparison of each damping method—constant damping $c = 60$ Ns/m and $c = 20$ Ns/m and variable damping $c = F_{\text{std}}/|\dot{x}|$, respectively. The damper graph shows the relation between virtual damping and velocity. As shown in the graph, maximum and minimum damping exhibit constant values independent of the velocity. In contrast, variable damping corresponds to a shift from maximum damping to minimum damping.

The bottom graph of Fig. 1(a) shows the minimum force to maintain the velocity with each case of damping methods. For example, if an operator wants to set the velocity at 0.1 m/s, the operator should use a minimum force corresponding to 6 N in the case of maximum damping, 2 N in the case of minimum damping, and 2 N in the case of variable damping with $F_{\text{std}} = 2$. The minimum force of variable damping maintains the standard force when the velocity falls in area B of the graph. Variable damping follows maximum damping when the standard force equals $F_{\text{std}} = 2$ N in area A. With respect to area B, variable damping changes from maximum damping to minimum damping. With respect to area C, variable damping follows minimum damping. With respect to areas A and C, the minimum force of variable damping increases when the velocity increases. With respect to area B, the minimum force of variable damping makes the operator change the velocity with the near-standard force.

In the bottom graph of Fig. 1(b), the right y axis denotes a time history of the desired velocity. For 5 s, the velocity trajectory changes from 0 to 0.15 m/s and back to 0 m/s. Subsequently, the left y axis shows the required force to ensure the velocity

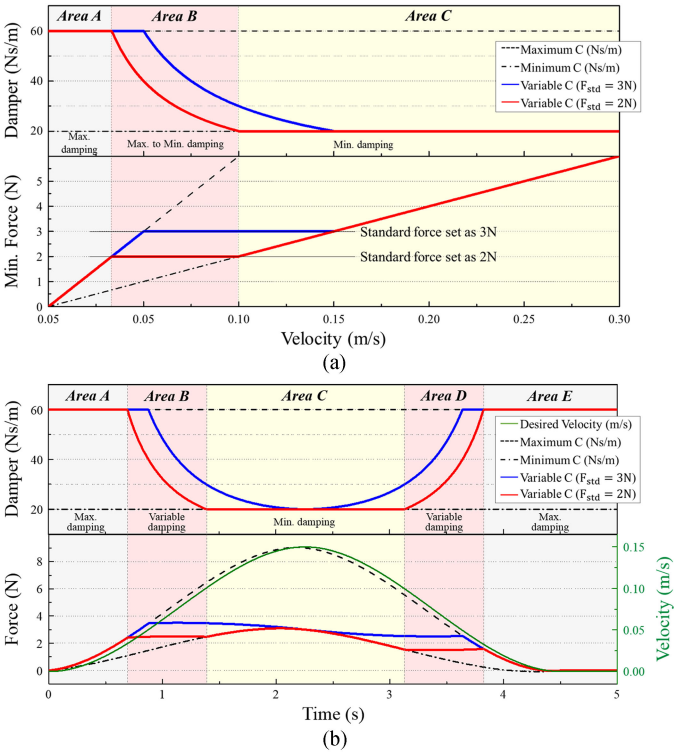

Fig. 1. Variable damping for a single-dimensional system: (a) virtual damping and responding minimum force relative to the velocity and (b) time history of the force and damping to follow the velocity trajectory.

trajectory for each case of damping methods. With respect to constant damping, the required force changes in a manner similar to the velocity trajectory. To obtain 0.15 m/s velocity with the maximum damping case, the operator should use a force exceeding 9 N. However, with respect to variable damping, the required force does not exceed 4 N to obtain the peak velocity.

When the standard force $F_{\text{std}} = 2$ N in areas A and E of the graph, the required force of variable damping follows those of the maximum damping to increase the required force. In area C, the required force of variable damping follows those of the minimum damping to decrease the required force. In areas B and D, variable damping changes between the maximum and minimum damping and the required force is close to the standard force. In area B, the required force exceeds the standard force to increase the velocity for acceleration. In contrast, in area D, the required force is less than the standard force to decrease the velocity for deceleration.

As mentioned, the proposed variable damping maintains the applied force as a standard force as much as possible. The value of variable damping applies maximum damping for fine movement and minimum damping for fast movement. Moreover, suggested variable damping includes adaptive parameters and it can be easily changed by the operator. The standard force is adjusted by the operator after selecting the maximum and minimum damping. Subsequently, the suggested method ensures that the required force is close to the standard force.

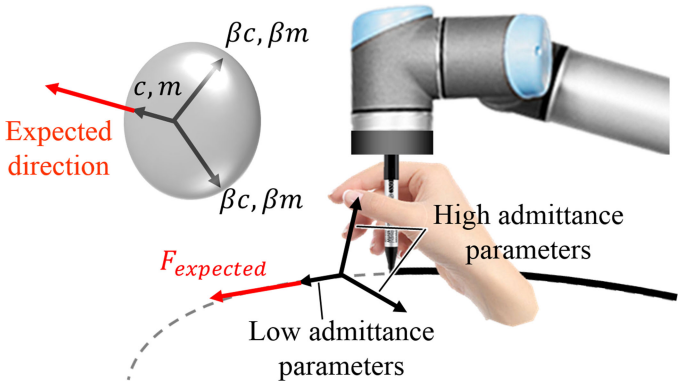

Fig. 2. Scheme of variable admittance for indirect intention.

IV. Variable Admittance for Indirect Intention

Variable admittance control guarantees both intuitiveness and accuracy through direct intention. However, unintended noise and mistakes that influence admittance control are also prevalent. To reduce disturbances during admittance control, an idea was proposed that involved guiding the robot along the expected path. Estimating indirect intention allows predicting the required force for the next direction. The robot then guides the linear and curve motion by changing the admittance around the expected direction. The proposed method is only applied to position movements.

Fig. 2 shows the basic scheme of the force guidance method. The expected force corresponds to the force that is necessary to continue the motion. The expected force has a certain direction when the operator interacts with a robot to move straight. If the robot can move easily toward a certain direction while the vertical direction is hard to move, then it reduces the disturbances due to a wrong force. Along the direction of the expected force, the admittance exhibits the default value. In contrast, the vertical direction of the expected force corresponds to a higher admittance parameter. Thus, vertical movements are smaller because higher admittance parameters make the maximum velocity lower and the response slower.

There are three steps for the force guidance method. In the first step, the indirect intention should be estimated in advance. A variable *reference variable* is introduced and filtered as an estimation of indirect intention. In the second step, the expected force is calculated with the filtered *reference variable*. Finally, the force guidance method is applied along the direction of the expected force.

A. Estimation of Indirect Intention

Prior to estimating indirect intention, it is assumed that indirect human intention corresponds to a curve on a plane with a constant curvature that includes the straight line. To ensure constant plane curvature, the curvature and unit binormal vector of the curve must possess constant values as given in the following:

$$\kappa \hat{\mathbf{B}} = \frac{1}{\rho} \hat{\mathbf{B}} = \text{constant} \tag{11}$$

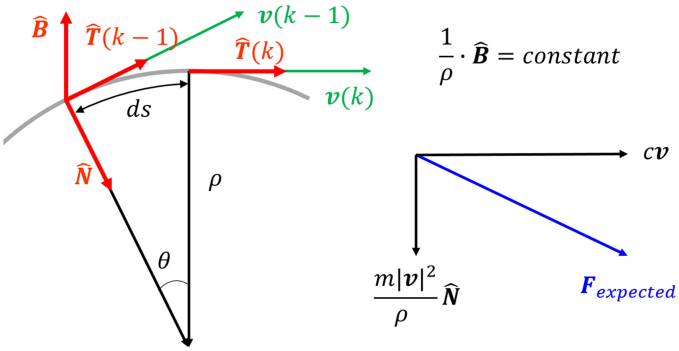

Fig. 3. Binormal vector of the curve and the expected force in the Cartesian space.

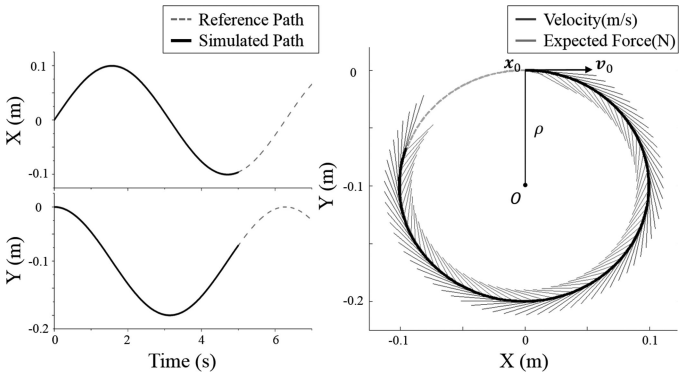

Fig. 4. Results of admittance control in which the input corresponds to the expected force.

where κ denotes a curvature and ρ denotes a radius of curvature. Additionally, $\hat{\mathbf{B}}$ denotes a binormal vector of the curve. Curvature times the unit binormal vector is defined as the *reference variable* in this study. The *reference variable* is calculated with the following equations.

As shown in Fig. 3, in the smooth curve motion, the unit binormal vector is calculated as follows

$$\hat{\mathbf{B}} = \frac{\hat{\mathbf{T}}(k) \times \hat{\mathbf{T}}(k-1)}{||\hat{\mathbf{T}}(k) \times \hat{\mathbf{T}}(k-1)||}. \tag{12}$$

Curvature is given by

$$\kappa = \left|\left|\frac{d\hat{\mathbf{T}}}{ds}\right|\right| = \frac{1}{||\mathbf{v}||}\left|\left|\frac{d\hat{\mathbf{T}}}{dt}\right|\right| = \frac{||\hat{\mathbf{T}}(k) - \hat{\mathbf{T}}(k-1)||}{||\mathbf{v}(k-1)||T} \tag{13}$$

where $\hat{\mathbf{T}}$ denotes a unit tangent vector. From the admittance control model, k denotes a time step and T denotes a period of the system. When the angle θ between $\hat{\mathbf{T}}(k)$ and $\hat{\mathbf{T}}(k-1)$ is sufficiently low, the following expression is obtained:

$$||\hat{\mathbf{T}}(k) \times \hat{\mathbf{T}}(k-1)|| = \sin\theta \approx ||\hat{\mathbf{T}}(k) - \hat{\mathbf{T}}(k-1)||. \tag{14}$$

In admittance control, the unit tangent vector is equal to the unit velocity vector. From (12)–(14), the *reference variable* is calculated as follows:

$$\frac{1}{\rho}\hat{\mathbf{B}}(k) = \frac{\hat{\mathbf{v}}(k) \times \hat{\mathbf{v}}(k-1)}{||\mathbf{v}(k-1)||T}. \tag{15}$$

During admittance control with straight or curve motion, it is necessary for the *reference variable* to include a constant vector. To expect the *reference variable* of the next time step, a low-pass filter is used as follows [24]:

$$\overline{\frac{1}{\rho}\hat{\mathbf{B}}}(k) = \alpha\overline{\frac{1}{\rho}\hat{\mathbf{B}}}(k-1) + (1-\alpha)\frac{1}{\rho}\hat{\mathbf{B}}(k) \tag{16}$$

where α represents the weighting factor.

B. Force Expectation

To guide the robot along the expected motion, the operator should force the robot to follow the expected force. The expected force is calculated as the sum of the centripetal force and the minimum driving force as follows:

$$F_{\text{expected}} = \frac{m|\mathbf{v}|^2}{\rho}\hat{\mathbf{N}} + c|\mathbf{v}|\hat{\mathbf{T}}. \tag{17}$$

A simulation is conducted on a plane to verify the calculation of the expected force. The initial conditions are given. The initial position corresponds to $\mathbf{x_o} = \{0, 0, 0\}$ m, and the initial velocity corresponds to $\mathbf{v_o} = \{0.1, 0, 0\}$ m/s. The virtual mass and damping correspond to $m = 10$ kg and $c = 20$ Ns/m, respectively. The radius of curvature is constant $\rho = 0.1$ m and the unit binormal vector also has a constant vector $\hat{\mathbf{B}} = \{0, 0, 1\}$. With the initial conditions, the expected force is calculated from (17) in each iteration.

The expected force is applied for 5 s, and the results are shown in Fig. 4. The graphs on the left show the time history of displacement along the x and y axes. The resulting path follows the reference path well. The graph on the right shows the path on the plane. The expected force is changed by the velocity vector and the *reference variable* in each iteration.

When the input force corresponds to the exact vector of the expected force, the resultant path follows the reference. The result indicates that if the operator can apply the expected force to the robot, the movement of the robot corresponds to a perfect line with a constant curvature.

C. Force Guidance Method

To ensure that the operator can control the force along the expected force, the force guidance method is suggested. From the force expectation, which was explained earlier, the expected force is obtained. The operator would apply a force along the direction of the expected force that implies the indirect intention of the operator. To guide the direction of the expected force, we set higher admittance parameters around that direction. If the x axis corresponds to the direction of the expected force, the virtual admittance parameters are changed as follows:

$$\mathbf{C} = \begin{bmatrix} c & 0 & 0 \\ 0 & \beta c & 0 \\ 0 & 0 & \beta c \end{bmatrix} \quad \mathbf{M} = \begin{bmatrix} m & 0 & 0 \\ 0 & \beta m & 0 \\ 0 & 0 & \beta m \end{bmatrix}. \tag{18}$$

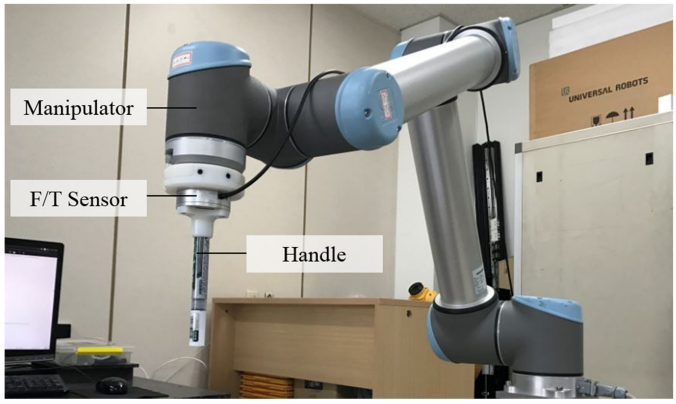

(a)

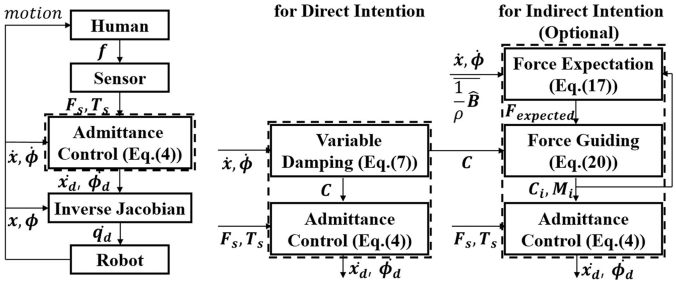

(b)

Fig. 5. Experimental setup: (a) hardware setup and (b) block diagram of the control scheme.

Around the x, y, and z axes, we set higher admittance parameters that increase in proportion to velocity as follows:

$$\beta = 1 + 10|\mathbf{v}| \tag{19}$$

where $\mathbf{C} \in \mathbb{R}^{3\times3}$ and $\mathbf{M} \in \mathbb{R}^{3\times3}$ denote damping and the mass matrix in the Cartesian space, respectively. Additionally, β represents a parameter that changes the vertical admittance, and β increases in proportion to velocity as can be seen from (19).

When the expected force corresponds to a random vector of the space, the frame is changed. The x axis changes with respect to the direction of the expected force and $\mathbf{R} \in \mathbb{R}^{3\times3}$ denotes the rotation matrix. Finally, virtual admittance relative to the expected force is calculated as follows:

$$\begin{aligned} \mathbf{C_i} &= \mathbf{RCR}^{-1} \\ \mathbf{M_i} &= \mathbf{RMR}^{-1} \end{aligned} \tag{20}$$

where $\mathbf{C_i} \in \mathbb{R}^{3\times3}$ and $\mathbf{M_i} \in \mathbb{R}^{3\times3}$ denote virtual damping and the mass matrix for indirect intention, respectively.

V. Experiments

A. Experimental Setup

As shown in Fig. 5(a), the experimental system consists of a six-DOF industrial manipulator (UR10, Universal Robot) and a six-axis force/torque sensor (RFT60-HA, Robotous) [25], [26]. The force/torque sensor is attached at the end effector of the manipulator. The manipulator is controlled by a control box obtained from Universal Robots and has a sampling period of 8 ms. Using another computer, sensor data are obtained at 200 Hz by using a low-pass filter.

Fig. 5(b) shows the control scheme of the experiments. The human controls the velocity by applying the force to the sensor attached to the end effector of the manipulator. Cartesian velocity and angular velocity are obtained based on variable admittance control. The inverse Jacobian matrix changes Cartesian and angular velocities to joint angular velocity and then sends the command to the real robot.

Variable admittance for direct intention is applied according to (7) in the position and orientation space. Both intuitiveness and accuracy are improved through variable admittance for direct intention. Conversely, with respect to indirect intention, variable admittance is only applied to the position space and improves the accuracy of motion by assisting the operator. Additionally, the indirect intention of the human is assumed as a curve on a plane with a constant curvature, and it limits the free motion. Therefore, with respect to a specific task, variable admittance for indirect intention could exhibit the best performance.

The evaluation of the physical human–robot interaction is a challenging problem. The interaction between the human and the robot depends on each task. In previous studies, a three-dimensional trajectory task was employed [14]. The evaluation of the pure interactions was better although the accuracy was not sufficient. Other studies performed drawing tasks [15], [16]. The time and accuracy were quantified. However, it is necessary to consider the interaction with the plane. In this study, tracking tasks were performed to verify the proposed algorithms. With respect to a spatial path, the pure interactions were evaluated and the time and accuracy were sufficiently quantified as well.

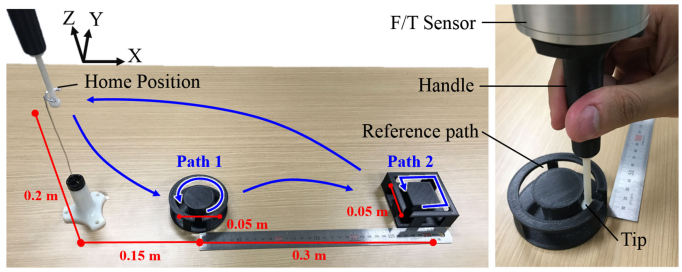

Fig. 6. Task setup with the home position and two reference paths. Path 1 is circular, while path 2 is rectangular.

B. Experimental Task

To verify admittance control, experimental tasks were performed by the operator. The task consists of three free motions and two tracking motions. The operator starts the robot from the home position, passes it through two reference paths, and then moves the robot to the home position as shown in Fig. 6. Reference paths correspond to circular and rectangular paths and represent curve motion and straight motion, respectively. The home position and the two reference paths are aligned along the x axis. The height of the home position corresponds

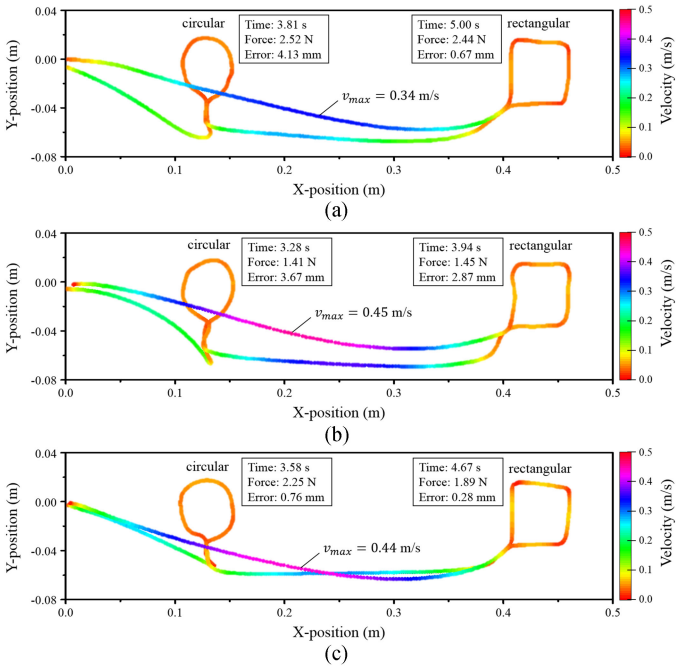

Fig. 7. Examples of the experimental task. The tasks are conducted with three different admittance: (a) maximum damping; (b) minimum damping; and (c) variable damping. The path followed through human–robot cooperation is illustrated along with the responding velocity.

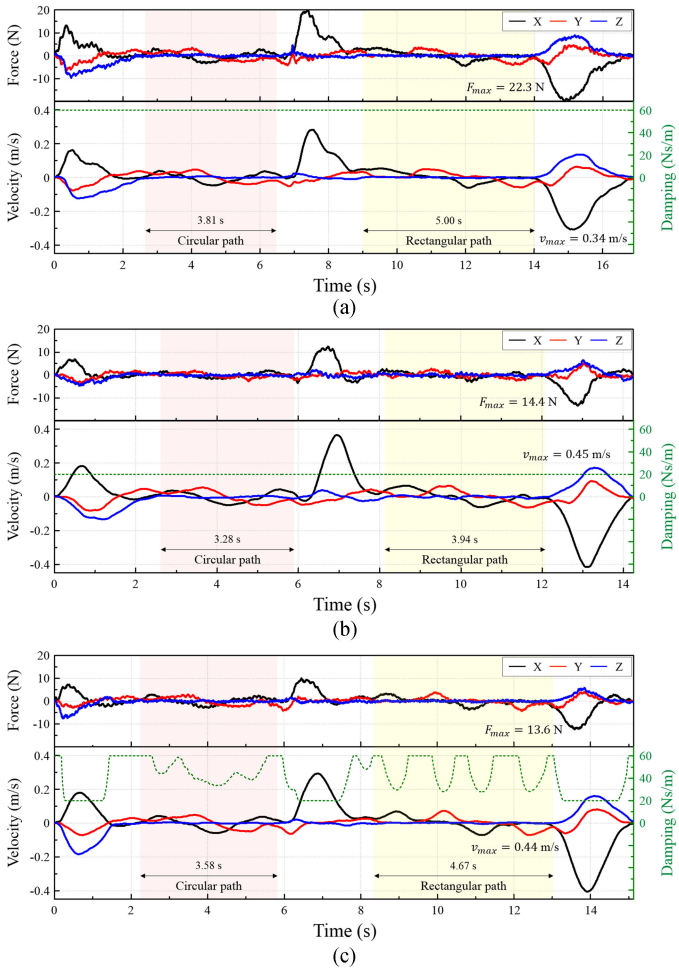

Fig. 8. Examples corresponding to three different admittances: (a) maximum damping; (b) minimum damping; and (c) variable damping. Graphs of applied force, measured velocity, and applied damping versus time are shown.

to 0.2 m. The distance between home and the circular path is 0.15 m. The distance between the circular and rectangular path is 0.3 m. The diameter of the circular path and a side length of the square are set as 0.05 m.

The operator is asked to move the tip to the reference paths and to track inside the reference paths. During the tracking motion, the tip should not contact the reference path and move as fast as possible. Tracking tasks were performed by five subjects with ages ranging from 23 to 31 years old. The operator practiced for 5 min prior to the experiments. After the practice, the operator repeated the tasks five times with each admittance control method. Each admittance control action was performed twenty-five times in total with five different subjects. The iteration time, applied force, and position information were recorded.

VI. Results and Discussions

To evaluate the admittance control for direct intention, the following three admittance controls were compared—two constant admittance controls with maximum and minimum damping and one variable admittance control. Graphical results were obtained and statistic results were compared using t-test. To verify the variable admittance for indirect intention, two variable admittance control were compared without and with force guidance. The effectiveness of force guidance was discussed in terms of smoothness of interaction.

A. Results for Direct Intention

In Fig. 7, examples with a single subject are illustrated with each damping case. The path followed through human–robot cooperation is illustrated with the responding velocity. The task time was measured from the starting moment to the stop moment, when the velocity is zero. The mean force corresponded to the average force calculated with the normal value of the applied force. The task completion time and the mean force exhibited an inverse relationship because high force reduces the time of a task with a high velocity. In addition, the error corresponds to the difference between the reference length and the recorded length traveled by the robot during the tracking motion.

For more details, the responding applied force, velocity, and damping are shown in Fig. 8. In Fig. 8(a) and (b), maximum damping exhibited higher values for the task time and force and minimum damping displayed a higher value for the velocity. In Fig. 8(c), damping was changed with the proposed method. In the free motions, minimum damping was experienced. In the tracking motions, damping varied to increase the accuracy and the velocity.

Fig. 9 shows the statistic results of the experimental task. The result showed that the maximum damping exhibited values as high as 21.17 s for the task time and 4.19 N for the mean force. The task time of the variable damping displayed results similar

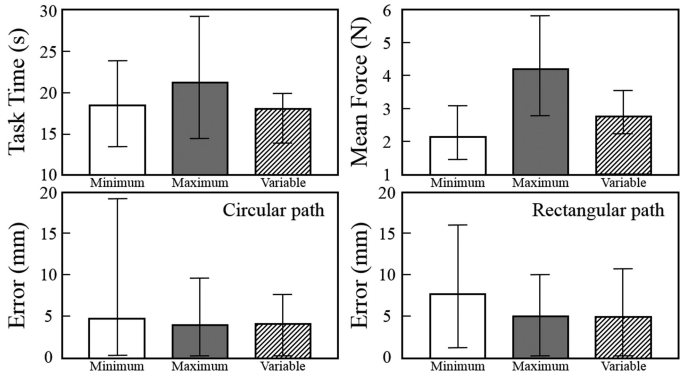

Fig. 9. Results of the experimental task. Three different admittance controls are compared for the task execution time, mean force, and error of the reference paths. The maximum value and the minimum value of each admittance control are illustrated.

TABLE I
t-TEST RESULTS OF THE EXPERIMENTAL TASKS

	Minimum const.	Maximum const.
Time	h = 0	h = 1
	(p=0.2835)	(p=0.0004)
Length	h = 1	h = 0
(circular path)	(p=0.0277)	(p=0.1570)
Length	h = 1	h = 0
(rectangular path)	(p=0.0235)	(p=0.3940)

to those of minimum damping including 17.99 and 18.42 s. The mean force of the variable damping corresponded to 2.76 N. This was faster than that of maximum damping although it was slightly slower than that of minimum damping.

In the tracking motions, minimum damping exhibited high errors with respect to the circular and rectangular paths at 4.79 and 7.72 mm, respectively. In contrast, maximum and variable damping displayed lower errors for the circular path at 4.02 and 3.79 mm, respectively. For the rectangular path, errors of 5.04 and 4.94 mm were obtained.

From the experimental results, a t-test was performed as shown in Table I. Variable damping was compared with the two constant damping values. When the variable h is one, the difference between variable damping and the compared constant damping is statistically significant. With respect to the execution time, the improvement of variable damping with respect to the maximum constant damping is statistically significant. Furthermore, with respect to the length of the reference paths, variable damping exhibited a significant difference with respect to the minimum constant damping. Given the variable damping for direct intention, the accuracy of the minimum constant damping and the task time of the maximum constant damping improved and were statistically significant. As a result, the advantage of using maximum damping for accuracy and minimum damping for task time is achieved by variable damping.

B. Results for Indirect Intention

As shown in Fig. 10 and Table II, the variable admittance that included indirect intention displayed results similar to those of

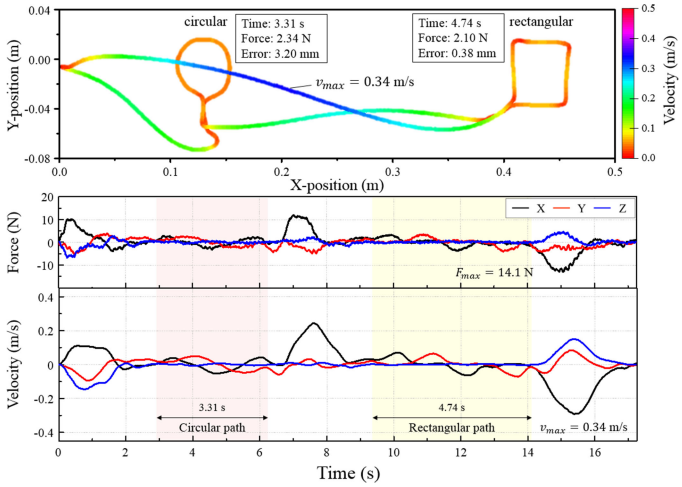

Fig. 10. Examples of the experimental task with force guidance. The cooperated path and the corresponding graphs.

TABLE II
COMPARISON OF THE FORCE GUIDANCE

	w/o Force guidance	w/ Force guidance
Task time (s)		
- circular path	4.12672	4.54432
- rectangular path	4.98016	5.79328
Mean force (N)		
- circular path	2.10605	2.00485
- rectangular path	2.02885	1.92706
Length error (mm)		
- circular path	3.79322	3.21897
- rectangular path	4.94223	4.85523
Mean squared jerk		
- circular path	1.16653E-05	0.56895E-05
- rectangular path	1.06721E-05	0.61018E-05

the variable damping for direct intention. During free motion, the task time corresponded to a slightly longer duration because of the disturbance due to the high admittance parameters. In contrast, with regard to tracking motion, the task time and mean force had a negligibly small difference with and without force guidance. Additionally, the accuracy slightly improved owing to the guidance but still had a small difference. The difference between the two admittance values was clearly verified with respect to the smoothness of movement.

The quantitative value of smoothness analyzed using mean-squared jerk [27] is utilized. Jerk, the time derivative of acceleration, has been used as an empirical measure of smoothness of movement. The mean-squared jerk is defined as

$$J = \frac{1}{t_2 - t_1} \int_{t_1}^{t_2} \dddot{x}(t)^2 dt. \tag{21}$$

Smaller values of J indicate better performance with respect to the smoothness of movement. As shown in Table II, the results of mean-squared jerk are compared. In both tracking motions, force guidance significantly improves the smoothness of the motion. The value of mean-squared jerk was reduced to almost half with force guidance. These results showed that

force guidance assists the operator by guiding the robot along the expected path to follow indirect intentions.

C. Discussions

The results showed clear improvements in task completion time and accuracy compared to the case of constant admittance control. Other similar schemes in [15] and [16] may yield similar results. However, these schemes require empirical coefficients (α, β [15], a, b [16]) that must be tuned to the hardware system. In contrast, in the proposed scheme, the concept of standard force makes variable damping applicable to other hardware.

However, the stability of the manipulator is still hardware dependent because nonlinear hardware characteristics change depending on the work environment and robot hardware. In this study, the boundary limit of the admittance parameters is heuristically or analytically obtained. Especially, the lower bound of the admittance parameters is associated with stability issues. Therefore, a general solution is needed to obtain admittance parameters that ensure the stability of the manipulator depending on the changing environment. This is one of the issues to be solved in future works.

Based on the variable damping for direct intention, the variable admittance for indirect intention was additionally applied. In the tracking motion, force guidance shows a significant improvement in the smoothness of the motion by comparing the value of mean-squared jerk. In the previous studies, predefined paths, regions, and environments were considered as indirect human intentions. In contrast, in this study, the operator can be assisted online by estimating indirect human intentions. This implies that the human–robot interaction improves the ability of the human. However, like in previous studies, there is a limit to the force guidance that robots cannot move as in free motion.

The estimation of indirect intention is another important issue. In the experiments, indirect intention was assumed as a curve on a plane with constant curvature. This assumption allows the robot to guide the human only on the plane surface. However, during the physical human–robot interaction, the intention of the human can be extended to various fields. For example, complex curve motion in industrial applications, constrained motion in robotic surgery, and exoskeleton motion for workers and patients can be improved by a proper estimation of indirect intention. In each case, indirect intention can be properly estimated by assuming certain conditions. As a result, the robot can be made to aid the human in a wide range of tasks.

VII. Conclusion

In this study, two variable admittance controls were introduced based on human intention. In direct intention, variable admittance led to improvements with respect to completion time and accuracy. The proposed standard force makes an operator adjust his/her own comfort force. With respect to the admittance variation, the operator controls the velocity with a similar value of the interacting force. Additionally, based on variable damping for direct intention, the indirect intention of a human is newly introduced to assist the human. To estimate the indirect intention, the *reference variable* is introduced and filtered. The estimation allows for the prediction of the next motion of the interaction and obtains an expectation of the next force. The variable admittance guides the direction of the expected force to compensate for noise and human errors.

The effectiveness of the proposed control schemes was verified by experiments. The experimental task, consisting of free motions and reference paths, was performed by five subjects. With respect to the direct intention, the results indicated that variable admittance performed better with respect to the execution time and the accuracy when compared with constant admittance. Additionally, with respect to the indirect intention, the variable admittance was verified by comparing the mean-squared jerk with or without force guidance.

Consequently, the results showed that the proposed variable admittance improves the capability of human–robot interactions.

References

[1] N. Hogan, "Impedance control: An approach to manipulation," in *Proc. IEEE Amer. Control Conf.*, 1984, vol. 107, pp. 304–313.

[2] A. Calanca, R. Muradore, and P. Fiorini, "A review of algorithms for compliant control of stiff and fixed-compliance robots," *IEEE/ASME Trans. Mechatronics*, vol. 21, no. 2, pp. 613–624, Apr. 2016.

[3] C. Passenberg, A. Peer, and M. Buss, "A survey of environment-, operator-, and task-adapted controllers for teleoperation systems," *Mechatronics*, vol. 20, no. 7, pp. 787–801, 2010.

[4] L. J. Love and W. J. Book, "Force reflecting teleoperation with adaptive impedance control," *IEEE Trans. Syst., Man, Cybern. B, Cybern.*, vol. 34, no. 1, pp. 159–165, Feb. 2004.

[5] J. Abbott, P. Marayong, and A. Okamura, "Haptic virtual fixtures for robot-assisted manipulation," *Robot. Res.*, vol. 28, pp. 49–64, 2007.

[6] E. Colgate and N. Hogan, "An analysis of contact instability in terms of passive physical equivalents," in *Proc. IEEE Int. Conf. Robot. Autom.*, 1989, pp. 404–409.

[7] E. Colgate and N. Hogan, "Robust control of dynamically interacting systems," *Int. J. Control*, vol. 1, pp. 65–88, 1988.

[8] M. Rahman, R. Ikeura, and K. Mizutani, "Investigating the impedance characteristic of human arm for development of robots to co-operate with human operators," in *Proc. IEEE Int. Conf. Syst., Man, Cybern.*, 1999, pp. 676–681.

[9] Y. Li and S. Ge, "Human-robot collaboration based on motion intention estimation," *IEEE/ASME Trans. Mechatronics*, vol. 19, no. 3, pp. 1007–1014, Jun. 2014.

[10] V. Duchaine and C. Gosselin, "Investigation of human-robot interaction stability using Lyapunov theory," in *Proc. IEEE Int. Conf. Robot. Autom.*, 2008, pp. 2189–2194.

[11] F. Dimeas and N. Aspragathos, "Reinforcement learning of variable admittance control for human-robot co-manipulation," in *Proc. IEEE/RSJ Int. Conf. Intell. Robots Syst.*, 2015, pp. 1011–1016.

[12] Y. Maeda, T. Hara, and T. Arai, "Human– robot cooperative manipulation with motion estimation," in *Proc. IEEE/RSJ Int. Conf. Intell. Robots Syst.*, 2001, pp. 2240–2245.

[13] F. Dimeas and N. Aspragathos, "Fuzzy learning variable admittance control for human– robot cooperation," in *Proc. IEEE/RSJ Int. Conf. Intell. Robots Syst.*, 2014, pp. 4770–4775.

[14] S. Grafakos, F. Dimeas, and N. Aspragathos, "Variable admittance control in pHRI using EMG-based arm muscles co-activation," in *Proc. IEEE Int. Conf. Syst., Man, Cybern.*, 2016, pp. 1900–1905.

[15] A. Lecours, B. Mayer-St-Onge, and C. Gosselin, "Variable admittance control of a four-degree-of-freedom intelligent assist device," in *Proc. IEEE Int. Conf. Robot. Autom.*, 2012, pp. 3903–3908.

[16] F. Ficuciello, L. Villani, and B. Siciliano, "Variable impedance control of redundant manipulators for intuitive human-robot physical interaction," *IEEE Trans. Robot.*, vol. 31, no. 4, pp. 850–863, Aug. 2015.

[17] P. Marayong and A. Okamura, "Speed-accuracy characteristics of human–machine cooperative manipulation using virtual fixtures with variable admittance," *Human Factors*, vol. 46, no. 3, pp. 518–532, 2004.

[18] F. Rydn, H. J. Chizeck, S. N. Kosari, H. King, and B. Hannaford, "Using kinect and a haptic interface for implementation of real-time virtual fixtures," in *Proc. 2nd Workshop RGB-D: Adv. Reasoning Depth Cameras*, 2011.
[19] P. Aigner and B. McCarragher, "Human integration into robot control utilising potential fields," in *Proc. IEEE Int. Conf. Robot. Autom.*, 1997, pp. 291–296.
[20] R. Ikeura, H. Monden, and H. Inooka, "Cooperative motion control of a robot and a human," in *Proc. IEEE Int. Conf. Robot Human Commun.*, 1994, pp. 112–117.
[21] T. Tsumugiwa, Y. Fuchikami, A. Kamiyoshi, R. Yokogawa, and K. Yoshida, "Stability analysis for impedance control of robot in human–robot cooperative task system," *Int. J. Adv. Mech. Des., Syst., Manuf.*, vol. 1, no. 1, pp. 113–121, 2007.
[22] A. Lecours, M. J. Otis, and C. Gosselin, "Modeling of physical human-robot interaction: Admittance controllers applied to intelligent assist devices with large payload," *Int. J. Adv. Robot. Syst.*, vol. 13, no. 5, pp. 1–12, 2016.
[23] Z. Wang, A. Peer, and M. Buss, "An HMM approach to realistic haptic human-robot interaction," in *Proc. 3rd Joint Eurohaptics Conf. Symp. Haptic Interf. Virtual Environ. Teleoper. Syst.*, 2009, pp. 374–379.
[24] J. M. Lucas and M. S. Saccucci, "Exponentially weighted moving average control schemes: Properties and enhancements," *J. Technometrics*, vol. 32, no. 1, pp. 1–12, 1990.
[25] UR10, Universal Robot. Accessed: July 20, 2017. [Online]. Available: https://www.universal-robots.com
[26] RFT60-HA, Robotous. Accessed: July 20, 2017. [Online]. Available: https://www.robotous.com/forcetorquesensor
[27] N. Hogan and D. Sternad, "Sensitivity of smoothness measures to movement duration, amplitude, and arrests," *J. Motor Behavior*, vol. 41, no. 6, pp. 529–534, 2009.

Gitae Kang received the B.S. degree in mechanical engineering from Sungkyunkwan University, Suwon, South Korea, in 2013. He is currently working toward the Ph.D. degree at the School of Mechanical Engineering, Sungkyunkwan University.

Since 2013, he has been with the Robotics Innovatory Laboratory, School of Mechanical Engineering, Sungkyunkwan University. His research interests include motion planning and human–robot interaction of a manipulator.

Hyun Seok Oh received the B.S. degree in mechanical engineering from Halla University, Wonju, South Korea, in 2016. He is currently working toward the Ph.D. degree at the School of Mechanical Engineering, Sungkyunkwan University, Suwon, South Korea.

Since 2016, he has been with the Robotics Innovatory Laboratory, School of Mechanical Engineering, Sungkyunkwan University. His research interests include robot hand control and machine learning.

Joon Kyue Seo received the B.S. degree in mechanical engineering from Sungkyunkwan University, Suwon, South Korea, in 2015. He is currently working toward the M.S. degree at the School of Mechanical Engineering, Sungkyunkwan University.

Since 2015, he has been with the Robotics Innovatory Laboratory, School of Mechanical Engineering, Sungkyunkwan University. His research interests include robot hands, manipulators, and machine learning with vision sensors.

Uikyum Kim received the B.S. degree in mechanical engineering from Sungkyunkwan University, Suwon, South Korea, in 2011, where he is currently working toward the Ph.D. degree at the School of Mechanical Engineering.

Since 2011, he has been with the Robotics Innovatory Laboratory, School of Mechanical Engineering, Sungkyunkwan University. His research interests include surgical robotics, force/tactile sensors for robotics applications, haptic interfaces, force-feedback control systems, dexterous manipulators for industrial robotics, soft robotics, and computing algorithms.

Hyouk Ryeol Choi (F'19) received the B.S. degree from Seoul National University, Seoul, South Korea, the M.S. degree from the Korea Advanced Institute of Science and Technology, Daejeon, South Korea, and the Ph.D. degree from Pohang University of Science and Technology, Pohang, South Korea, all in mechanical engineering, in 1984, 1986, and 1994, respectively.

From 1986 to 1989, he served as an Associate Research Engineer with the IT Research Center, LG electronics. From 1993 to 1995, he was a Postdoctoral Researcher with Kyoto University, Kyoto, Japan. From 1999 to 2000, he was a JSPS Fellow with the National Institute of Advanced Industrial Science and Technology, Japan. Additionally, from 2008 to 2009, he was a Visiting Professor with the University of Washington, Seattle, WA, USA. Since 1995, he has been a Full-Time Professor with the School of Mechanical Engineering, Sungkyunkwan University, Suwon, South Korea. His research interests include soft robotics, robotic mechanisms, field applications of robots, dexterous robotic hands, and manipulation.

Dr. Choi was an Editor for the *International Journal of Control, Automation, and Systems*. He is currently a Technical Editor for the IEEE/ASME TRANSACTIONS ON MECHATRONICS, and the Senior Editor for the *Journal of Intelligent Service Robotics*. He serves as a Co-Chair of the IEEE RAS Technical Committee "Robot Hand, Grasping and Manipulation." He was the General Chair of the 2012 IEEE Conference on Automation Science and Engineering, Seoul.